COMPDYN 2015
5th ECCOMAS Thematic Conference on
Computational Methods in Structural Dynamics and Earthquake Engineering
M. Papadrakakis, V. Papadopoulos, V. Plevris (eds.)
Crete Island, Greece, 25–27 May 2015

SIMPLIFIED MODEL FOR COUPLED VIBRATION OF ADJACENT STRIP FOOTINGS

Jue Wang[1] , Ding Zhou[2] , Weiqing Liu[3]

[1,2,3] College of Civil Engineering, Nanjing Tech University, Nanjing 211816, P. R. China
e-mail: [1]wjatnjut@gmail.com; [2]dingzhou57@yahoo.com; [3]wqliu@njut.edu.cn

Keywords: foundation-soil-foundation interaction, impedance function, lateral-rocking dynamic, elastic half-space, Green function

Abstract. *A semi-analytical procedure is presented to obtain the coupling lateral-rocking impedances between adjacent strip footings rested on an elastic half space. The interfaces between the footings and the supporting medium are divided into a number of strip elements. Asymmetrical Green functions of the elastic soil medium under lateral and vertical harmonic uniform excitation with infinite length are derived to establish the dynamic-flexibility matric for those strip elements. The intensities of such forces are adjusted so the displacement of the elements are compatible with the rigid body translations or rotations of the footings. The coupled lateral-rocking impedances are solved by adding the bending moments and the contact forces on each element. The accuracy is verified by the comparison study with the rigorous results from the mix-boundary-value method. The influence of the distance ratio S/L on the dynamic cross interaction (DCI) effect between adjacent footings is discussed in detail. It is shown that the lateral-rocking interaction between adjacent strip footings should be taken into consideration when* S/L *less than 5.0.*

1 INTRODUCTION

The substructure method, which enables soil and structure to be considered separately, is widely applied in the Soil-structure interaction (SSI). In practical situations, structures are sometimes placed close to each other due to a limitation of space. Hence, in the realistic evaluation of their dynamic characteristics, it is necessary to consider not only the interaction between the footing and the soil medium but also the interaction between adjacent footings through the soil, which is known as dynamic cross interaction (DCI) problem. Besides experimental investigations and numerical procedures, substructure method is still a powerful and feasible approach to DCI problems. In the substructure method, an important step is the computation of the footing impedances with the consideration of DCI effect.

The analytical solution for footing impedance can be obtained through a stress boundary-value method, which is based on assumptions about stress distributions (static rigidity, uniform, parabolic or their combinations) underneath the footing [1, 2]. However, as the assumed distribution may not satisfy the contact conditions at the footing-soil interface for adjacent footings, the deflected shape of the interface has to be modified based on the averaging techniques. Warburton et al. [3] provided an approximate method based on the relaxed contact assumption to study the dynamic response of two rigid circular footings on soil medium. More rigorous solutions for the impedance of footing can be obtained as a mixed boundary-value problem formulated in terms of dual integral equations [4, 5]. However, as the solutions of dual integral equations cannot be expressed by elementary functions, there are limitations to obtain the contact stress functions for a DCI problem. Otherwise, some semi-analytical approaches make the impedance solve flexibly [6-8]. Savidis and Richter [9] investigated the vertical cross-interference between two rigid, massless, smooth contacting surface footings by boundary integral equations in conjunction with constant elements in soil-footing interface. Dynamic interaction of a group of flexible strip footings resting on smooth contact with a homogeneous elastic half-space was studied by Wang et al. [10] based on a classical Green function for a concentrated vertical line load. It was extended later by Senjuntichai and Kaewjuea [11] to a multilayered poroelastic half-space. Their studies were limited to vertical dynamic interaction. However, the coupling lateral-rocking dynamic holds great significance for earthquake engineering as the largest effects of earthquake are on horizontal ground motion rather than vertical ground motion. In this paper, a discretization method is proposed to evaluate the coupling lateral-rocking impedance of adjacent strip footings intimately attached to an elastic half-space. The influence of the distance ratio S/L on the DCI effect between two footings is discussed in detail.

2 MODEL DESCRIPTION

The lateral-rocking oscillation of two adjacent strip footings with full contact to the free surface of an elastic half-space with different separation distance S is considered as shown in Fig. 1. Footing A with the width L_a is excited by the lateral excitation $P_a e^{i\omega t}$ and the rocking excitation $M_a e^{i\omega t}$. Footing B with the width L_b is excited by the lateral excitation $P_b e^{i\omega t}$ and the rocking excitation $M_b e^{i\omega t}$. For the strip footing such as track foundation, dam or building footing with a high ratio of length to width, it is reasonable to be simplified as a generalized plane strain problem. Considering DCI effect, the dynamic force and deformation relationship of the adjacent footings can be expressed by

$$\begin{Bmatrix} P_a \\ P_b \\ M_a \\ M_b \end{Bmatrix} = \begin{bmatrix} \Re_{\mathrm{hh}} & \Re_{\mathrm{hr}} \\ \Re_{\mathrm{rh}} & \Re_{\mathrm{rr}} \end{bmatrix} \begin{Bmatrix} U_a \\ U_b \\ \Theta_a \\ \Theta_b \end{Bmatrix} = [\Re] \begin{Bmatrix} U_a \\ U_b \\ \Theta_a \\ \Theta_b \end{Bmatrix} \tag{1}$$

where U_a and U_b are the lateral displacements of Footing A and B, respectively. Θ_a and Θ_b are rocking angles of corresponding footings. **[ℜ]** is the impedance matrix of the system consisting of lateral impedance $\Re_{\mathrm{hh}}$, rocking impedance $\Re_{\mathrm{rr}}$ and coupling impedance $\Re_{\mathrm{rh}}$. Each impedance in the **[ℜ]** is a complex number and can be interpreted as a spring with the frequency-dependent coefficient K(ω) and a dashpot in parallel with the frequency-dependent coefficient C(ω). Consequently, a simplified model, as shown in Fig. 2, can be built to simulate the coupled vibration of adjacent strip footings based on the impedance matrix **[ℜ]**.

For the simplification in analysis, the interfaces beneath Footing A and B are divided into *N* and *M* surface strip elements, respectively, as shown in Fig. 1. The widths of all the elements beneath Footing A and B are denoted by $\Delta_a=L_a/N$ and $\Delta_b=L_b/M$, respectively, where *N* and *M* represent the division number of Footing A and B. It is assumed that the *n*-th element (*n*=1，… ， *N*) beneath Footing A is subjected to a uniform lateral traction $p_n^{(a)}\mathrm{e}^{\mathrm{i}\omega t}$ and a vertical traction $q_n^{(a)}\mathrm{e}^{\mathrm{i}\omega t}$. Similarly, the *m*-th element (*m*=1，… ， *M*) beneath Footing B is subjected to a uniform lateral traction $p_m^{(b)}\mathrm{e}^{\mathrm{i}\omega t}$ and a vertical traction $q_m^{(b)}\mathrm{e}^{\mathrm{i}\omega t}$.

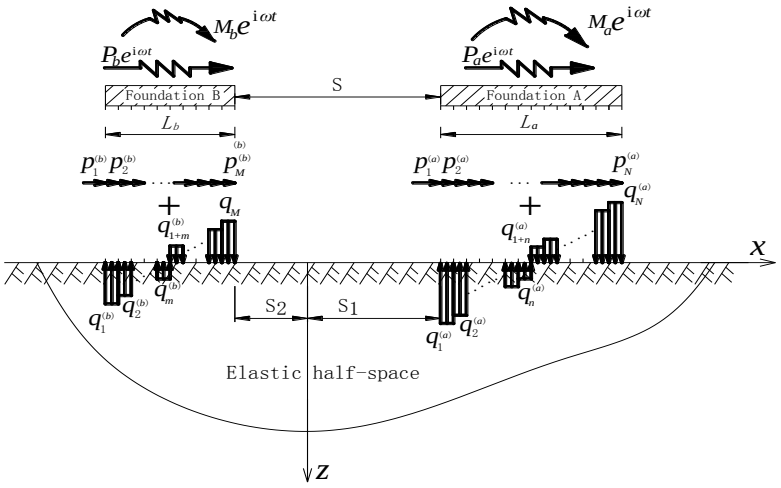

Fig. 1 The dynamic interaction model of the adjacent strip footings attached to an elastic half-space under lateral-rocking harmonic excitations

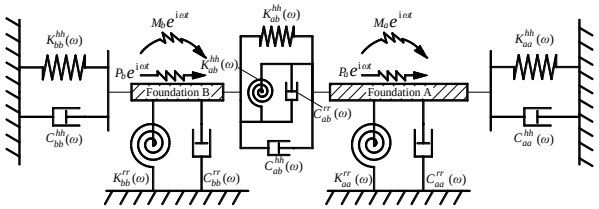

Fig. 2 Equivalent model of two adjacent footings under the lateral-rocking dynamic interaction

3 FORMULATION

3.1 The Half-space Green Function

Based on the Cartesian coordinate system (x-z) with z=0 at the free surface, the wave equations in an elastic half-space of homogeneous solid are given by

$$\begin{cases} (\lambda_s+G_s)\left(\dfrac{\partial^2 u(x,z,t)}{\partial x^2}+\dfrac{\partial^2 w(x,z,t)}{\partial x\partial z}\right)+G_s\nabla^2 u(x,z,t)=\rho_s\dfrac{\partial^2 u(x,z,t)}{\partial t^2} \\ (\lambda_s+G_s)\left(\dfrac{\partial^2 u(x,z,t)}{\partial x\partial z}+\dfrac{\partial^2 w(x,z,t)}{\partial z^2}\right)+G_s\nabla^2 w(x,z,t)=\rho_s\dfrac{\partial^2 w(x,z,t)}{\partial t^2} \end{cases} \tag{2}$$

where ρ_s is the density of the soil, G_s and λ_s are the Lam é constants. $\nabla^2=\left(\dfrac{\partial^2}{\partial x^2}+\dfrac{\partial^2}{\partial z^2}\right)$ denotes the Laplacian operator. u, w are the displacement components in x and z directions. As the footings are excited by harmonic forces, their steady-state vibrations satisfy $u(x, z, t)=U(x, z)e^{i\omega t}$, $w(x, z, t)=W(x, z)e^{i\omega t}$. For brevity, the time dependence $e^{i\omega t}$ is omitted.

Considering the unit lateral uniform traction applied at the interval [x_1, x_2], the boundary conditions at ground surface z=0 are given by

$$\sigma_{zz}(x,0)=0;\ \tau_{xz}(x,0)=\begin{cases}-e^{i\omega t} & x_1\le x\le x_2\\ 0 & \text{Other}\end{cases} \tag{3}$$

Considering the unit vertical uniform traction applied at the interval [x_1, x_2], the boundary conditions at ground surface z=0 are given by

$$\sigma_{zz}(x,0)=\begin{cases}-e^{i\omega t} & x_1\le x\le x_2\\ 0 & \text{Other}\end{cases};\quad \tau_{xz}(x,0)=0 \tag{4}$$

The general solutions of Eq. (2) for a half-space can be obtained by the method of separation of variable. The general solutions for stresses σ_{zz} and τ_{xz} can be obtained by the stress-displacement differential relationship. Based on the boundary condition of Eq. (3), the unknown coefficients in the general solutions can be determined. Therefore, the lateral and vertical displacement fields $G_{1,2}(x,0)$ and $G_{2,2}(x,0)$ due to the unit lateral uniform load are as follows

$$G_{1,1}(x,0)=-\frac{V_s}{\pi\omega G_s}\int_0^\infty\frac{\sqrt{\eta^2-1}}{\eta F(\eta)}\left\{\sin\left[\frac{\eta\omega}{V_s}(x-x_1)\right]-\sin\left[\frac{\eta\omega}{V_s}(x-x_2)\right]\right\}d\eta \tag{5}$$

$$G_{2,1}(x,0)=\frac{V_s}{\pi\omega G_s}\int_0^\infty\frac{\left(2\eta^2-1-2\sqrt{\eta^2-\vartheta^2}\sqrt{\eta^2-1}\right)}{F(\eta)}\left\{\cos\left[\frac{\eta\omega}{V_s}(x-x_1)\right]-\cos\left[\frac{\eta\omega}{V_s}(x-x_2)\right]\right\}d\eta \tag{6}$$

Similarly, the lateral and vertical surface displacements $G_{1,2}(x,0)$ and $G_{2,2}(x,0)$ due to the unit vertical uniform traction are as follows

$$G_{1,2}(x,0)=-G_{2,1}(x,0) \tag{7}$$

$$G_{2,2}(x,0)=-\frac{V_s}{\pi\omega G_s}\int_0^\infty\frac{\sqrt{\eta^2-\vartheta^2}}{\eta F(\eta)}\left\{\sin\left[\frac{\eta\omega}{V_s}(x-x_1)\right]-\sin\left[\frac{\eta\omega}{V_s}(x-x_2)\right]\right\}d\eta \tag{8}$$

In Eqs. (5-8), $\eta=\xi V_s/\omega$, $\vartheta=V_s/V_p$, $F(\eta)=(2\eta^2-1)^2-4\eta^2\sqrt{\eta^2-\vartheta^2}\sqrt{\eta^2-1}$, where ξ is the wave number, V_p is the dilatational wave (P wave) velocity with $V_p=\sqrt{(\lambda_s+2G_s)/\rho_s}$; V_s is the shear wave (S wave) velocity with $V_s=\sqrt{G_s/\rho_s}$.

3.2 Coupling Lateral-Rocking Impedance

Based on the superposition principle, the lateral displacement function $U(x,0)$ and the vertical displacement $W(x,0)$ due to the coupling lateral-rocking excitations on the footings are as follows

$$U(x,0)=\sum_{n=1}^{N}p_n^{(a)}G_{1,1}(x,0)+\sum_{m=1}^{M}p_m^{(b)}G_{1,1}(x,0)+\sum_{n=1}^{N}q_n^{(a)}G_{1,2}(x,0)+\sum_{m=1}^{M}p_m^{(a)}G_{1,2}(x,0) \tag{9}$$

$$W(x,0)=\sum_{n=1}^{N}p_n^{(a)}G_{2,1}(x,0)+\sum_{m=1}^{M}p_m^{(b)}G_{2,1}(x,0)+\sum_{n=1}^{N}q_n^{(a)}G_{2,2}(x,0)+\sum_{m=1}^{M}p_m^{(a)}G_{2,2}(x,0) \tag{10}$$

The following flexibility equation of the system can established as follows by substituting the central coordinate of each element into Eqs. (9) and (10)

$$\begin{bmatrix} \boldsymbol{A}_{N\times N}^{(1)} & \boldsymbol{B}_{N\times M}^{(1)} & \boldsymbol{C}_{N\times N}^{(1)} & \boldsymbol{D}_{N\times M}^{(1)} \\ \boldsymbol{A}_{M\times N}^{(2)} & \boldsymbol{B}_{M\times M}^{(2)} & \boldsymbol{C}_{M\times N}^{(2)} & \boldsymbol{D}_{M\times M}^{(2)} \\ \boldsymbol{A}_{N\times N}^{(3)} & \boldsymbol{B}_{N\times M}^{(3)} & \boldsymbol{C}_{N\times N}^{(3)} & \boldsymbol{D}_{N\times M}^{(3)} \\ \boldsymbol{A}_{M\times N}^{(4)} & \boldsymbol{B}_{M\times M}^{(4)} & \boldsymbol{C}_{M\times N}^{(4)} & \boldsymbol{D}_{M\times M}^{(4)} \end{bmatrix} \begin{Bmatrix} \hat{\boldsymbol{p}}^{(a)} \\ \hat{\boldsymbol{p}}^{(b)} \\ \hat{\boldsymbol{q}}^{(a)} \\ \hat{\boldsymbol{q}}^{(a)} \end{Bmatrix} = \begin{Bmatrix} \hat{\boldsymbol{U}}^{(a)} \\ \hat{\boldsymbol{U}}^{(b)} \\ \hat{\boldsymbol{W}}^{(a)} \\ \hat{\boldsymbol{W}}^{(a)} \end{Bmatrix} \tag{11}$$

in which, $\hat{\boldsymbol{p}}^{(a)}=\left\{p_1^{(a)},\ \cdots,\ p_N^{(a)}\right\}^T$; $\hat{\boldsymbol{p}}^{(b)}=\left\{p_1^{(b)},\ \cdots,\ p_M^{(b)}\right\}^T$; $\hat{\boldsymbol{q}}^{(a)}=\left\{q_1^{(a)},\ \cdots,\ q_N^{(a)}\right\}^T$; $\hat{\boldsymbol{q}}^{(b)}=\left\{q_1^{(b)},\ \cdots,\ q_M^{(b)}\right\}^T$; $\hat{\boldsymbol{U}}^{(a)}=\left\{U_1^{(a)},\ \cdots,\ U_N^{(a)}\right\}^T$; $\hat{\boldsymbol{U}}^{(b)}=\left\{U_1^{(b)},\ \cdots,\ U_M^{(b)}\right\}^T$; $\hat{\boldsymbol{W}}^{(a)}=\left\{\hat{W}_1^{(a)},\ \cdots,\ \hat{W}_N^{(a)}\right\}^T$; $\hat{\boldsymbol{W}}^{(b)}=\left\{W_1^{(b)},\ \cdots,\ W_M^{(b)}\right\}^T$. The expressions for every elements ($\boldsymbol{A}^{(i)}$, $\boldsymbol{B}^{(i)}$, $\boldsymbol{C}^{(i)}$, $\boldsymbol{D}^{(i)}$, $i\in1,2,3,4$) in the flexibility matrix are shown in the Appendix.

In consideration of the full contact between the rigid footings and the soil medium, the displacements of all the elements and footings should be satisfied as

$$\begin{Bmatrix} \hat{\boldsymbol{U}}^{(a)} \\ \hat{\boldsymbol{U}}^{(b)} \\ \hat{\boldsymbol{W}}^{(a)} \\ \hat{\boldsymbol{W}}^{(a)} \end{Bmatrix} = \begin{bmatrix} \hat{\boldsymbol{I}}_N & \hat{\boldsymbol{0}} & \hat{\boldsymbol{0}} & \hat{\boldsymbol{0}} \\ \hat{\boldsymbol{0}} & \hat{\boldsymbol{I}}_M & \hat{\boldsymbol{0}} & \hat{\boldsymbol{0}} \\ \hat{\boldsymbol{0}} & \hat{\boldsymbol{0}} & \hat{\boldsymbol{E}}_N & \hat{\boldsymbol{0}} \\ \hat{\boldsymbol{0}} & \hat{\boldsymbol{0}} & \hat{\boldsymbol{0}} & \hat{\boldsymbol{E}}_M \end{bmatrix} \begin{Bmatrix} U_a \\ U_b \\ \Theta_a \\ \Theta_b \end{Bmatrix} \tag{12}$$

where, $\hat{\boldsymbol{I}}_N=\underbrace{\{1,\cdots,1\}}_{N}^T$; $\hat{\boldsymbol{I}}_M=\underbrace{\{1,\cdots,1\}}_{M}^T$; $\hat{\boldsymbol{E}}_N=\left\{\frac{2n-1-N}{2N}L_a\right\}^T, n=1,\cdots,N$; $\hat{\boldsymbol{E}}_M=\left\{\frac{2m-1-M}{2M}L_b\right\}^T, m=1,\cdots,M$.

Equating the excitation and the contact tractions for Footing A and Footing B yields

$$\begin{Bmatrix} P_a \\ P_b \\ M_a \\ M_b \end{Bmatrix} = \begin{bmatrix} \Delta_a\hat{\boldsymbol{I}}_N & \hat{\boldsymbol{0}} & \hat{\boldsymbol{0}} & \hat{\boldsymbol{0}} \\ \hat{\boldsymbol{0}} & \Delta_b\hat{\boldsymbol{I}}_M & \hat{\boldsymbol{0}} & \hat{\boldsymbol{0}} \\ \hat{\boldsymbol{0}} & \hat{\boldsymbol{0}} & \Delta_a\hat{\boldsymbol{E}}_N & \hat{\boldsymbol{0}} \\ \hat{\boldsymbol{0}} & \hat{\boldsymbol{0}} & \hat{\boldsymbol{0}} & \Delta_b\hat{\boldsymbol{E}}_M \end{bmatrix}^T \begin{Bmatrix} \hat{\boldsymbol{p}}^{(a)} \\ \hat{\boldsymbol{p}}^{(b)} \\ \hat{\boldsymbol{q}}^{(a)} \\ \hat{\boldsymbol{q}}^{(a)} \end{Bmatrix} \tag{13}$$

Comparing the force-displacement relationship of Footing A and B, which can be established based on Eqs. (11-13), to the Eq. (1), the coupling lateral-rocking impedance matrix of adjacent footings can be obtained

$$[\mathfrak{R}]=\begin{bmatrix}\Delta_a\hat{\boldsymbol{I}}_N & \hat{\boldsymbol{0}} & \hat{\boldsymbol{0}} & \hat{\boldsymbol{0}}\\ \hat{\boldsymbol{0}} & \Delta_b\hat{\boldsymbol{I}}_M & \hat{\boldsymbol{0}} & \hat{\boldsymbol{0}}\\ \hat{\boldsymbol{0}} & \hat{\boldsymbol{0}} & \Delta_a\hat{\boldsymbol{E}}_N & \hat{\boldsymbol{0}}\\ \hat{\boldsymbol{0}} & \hat{\boldsymbol{0}} & \hat{\boldsymbol{0}} & \Delta_b\hat{\boldsymbol{E}}_M\end{bmatrix}^T\begin{bmatrix}\boldsymbol{A}^{(1)}_{N\times N} & \boldsymbol{B}^{(1)}_{N\times M} & \boldsymbol{C}^{(1)}_{N\times N} & \boldsymbol{D}^{(1)}_{N\times M}\\ \boldsymbol{A}^{(2)}_{M\times N} & \boldsymbol{B}^{(2)}_{M\times M} & \boldsymbol{C}^{(2)}_{M\times N} & \boldsymbol{D}^{(2)}_{M\times M}\\ \boldsymbol{A}^{(3)}_{N\times N} & \boldsymbol{B}^{(3)}_{N\times M} & \boldsymbol{C}^{(3)}_{N\times N} & \boldsymbol{D}^{(3)}_{N\times M}\\ \boldsymbol{A}^{(4)}_{M\times N} & \boldsymbol{B}^{(4)}_{M\times M} & \boldsymbol{C}^{(4)}_{M\times N} & \boldsymbol{D}^{(4)}_{M\times M}\end{bmatrix}^{-1}\begin{bmatrix}\hat{\boldsymbol{I}}_N & \hat{\boldsymbol{0}} & \hat{\boldsymbol{0}} & \hat{\boldsymbol{0}}\\ \hat{\boldsymbol{0}} & \hat{\boldsymbol{I}}_M & \hat{\boldsymbol{0}} & \hat{\boldsymbol{0}}\\ \hat{\boldsymbol{0}} & \hat{\boldsymbol{0}} & \hat{\boldsymbol{E}}_N & \hat{\boldsymbol{0}}\\ \hat{\boldsymbol{0}} & \hat{\boldsymbol{0}} & \hat{\boldsymbol{0}} & \hat{\boldsymbol{E}}_M\end{bmatrix} \quad (14)$$

4 NUMERICAL EXAMPLES AND DISCUSSIONS

4.1 Comparison Study

Luco and Westmann [4] solved the forced oscillations of a massless rigid strip footing with width L on half-space by using the mixed boundary-value approach. There are considerable difficulties in solving the integral equations numerically or analytically, therefore only a special case for Poisson's ratio ν=0.5 was studied rigorously. The cases with Poisson's ratio ν<0.5 were approximately studied by using the dominant part of the singular integral equation to evaluate the impedances of the strip footing, which is only valid for the low frequency $a_0\leq 1$. In order to compare with the Luco's solutions, the coupling lateral-rocking impedance matrix $\mathfrak{R}$ is transformed into the flexibility by $\boldsymbol{F}=\mathfrak{R}^{-1}$. The flexibility of the footing with respect to dimensionless exciting frequency is plotted in Figs. 3 and 4 for different Poisson's ratios ν=0.5, 0.25. In Figs. 3 and 4, the excellent agreements with Luco's solution approves the correctness and effectiveness of the present method. In addition, Fig. 4 also show that the present method covers a wider range of frequency than Luco's method.

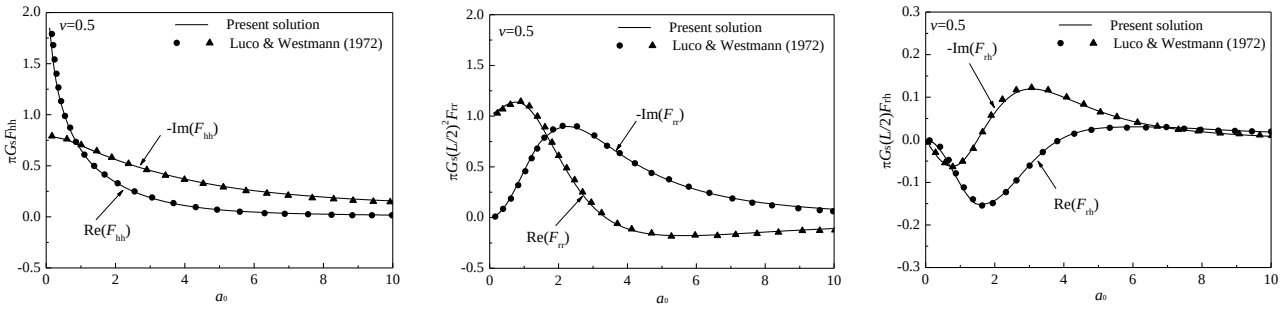

(a) (b) (c)

Fig. 3 Comparison of the present method with mixed boundary-value method for ν=0.5:
(a) Lateral; (b)Rocking; (c)Coupled lateral-rocking

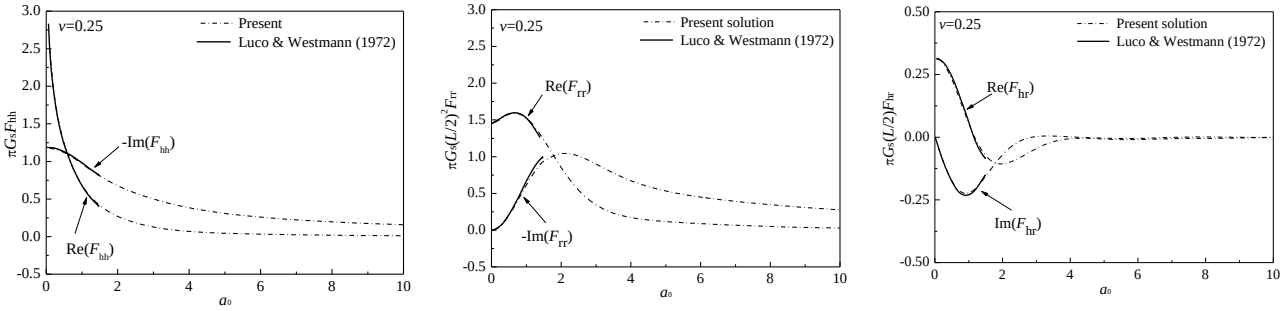

(a) (b) (c)

Fig. 4 Comparison of the present method with mixed boundary-value method for ν=0.25:
(a) Lateral; (b)Rocking; (c)Coupled lateral-rocking

4.2 Influence of the Distance Ratio on Impedances

Two identical strip footings subjected to harmonic lateral-rocking excitations are used to investigate the influence of the ratio between separation distance to footing width *S*/*L* on DCI effect. The variations of lateral and rocking impedances of a footing with respect to different distance ratios (*S*/*L*=0.125, 0.5, 3, 5, 10, ∞) are displayed in Figs. 5 and 6. It can be seen that the lateral and rocking impedances of two footings in the case of closely spaced distance ratio such as *S*/*L*=0.125 fluctuate around that of a single footing. In general, the DCI effect would make the impedances more frequency-dependent. Moreover, the influence from the adjacent footing is not significant in the case of large distance ratio such as *S*/*L*=5.0.

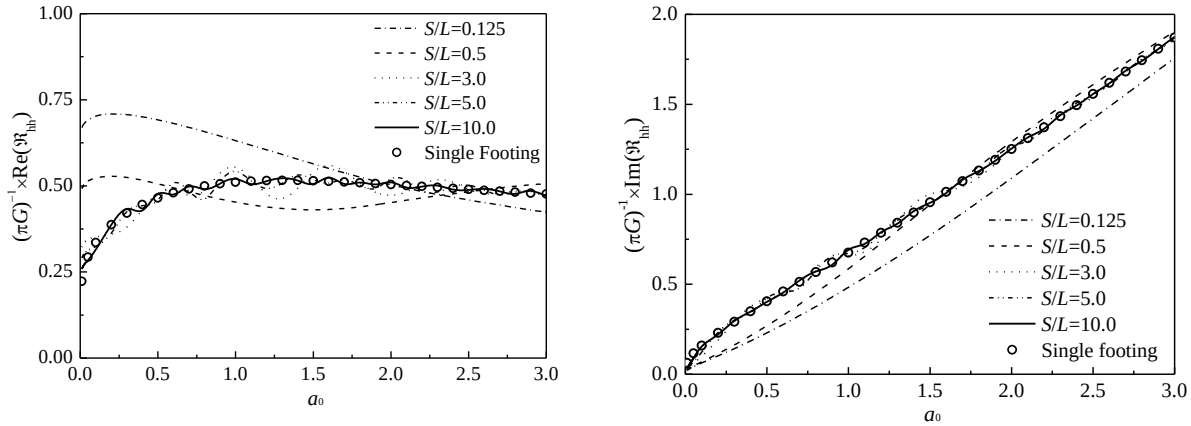

(a) (b)

Fig. 5 Lateral impedance $\mathfrak{R}_{hh}$ for different distance ratio *S*/*L*: (a) Stiffness; (b) Damping

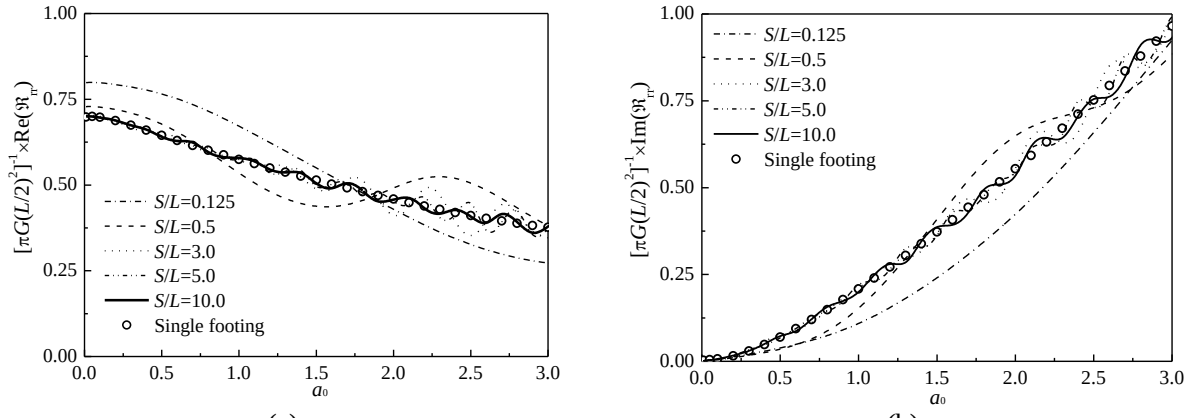

(a) (b)

Fig. 6 Rocking impedance $\mathfrak{R}_{rr}$ for different distance ratio *S*/*L*: (a) Stiffness; (b) Damping

5 CONCLUSION

An efficient semi-analytical method has been presented for obtaining the coupling lateral-rocking impedance of two adjacent footings. The accuracy is verified by the comparison study with the rigorous results from the mix-boundary-value method. Based on the parametric study on DCI effect, the distance ratio *S*/*L* between adjacent strip footings greatly influences the cross dynamic interaction especially for a small ratio less than 5.0. The approach has a definite physical meaning, and is easy to be mastered by technicians for dynamic analysis and seismic design of strip footings with close space, such as parallel tracks or adjacent buildings with a high ratio of length to width.

6 ACKNOWLEDGEMENTS

The financial supports from the Natural Science Foundation of Jiangsu Province, China (SBK201322459) are greatly acknowledged. This work is also supported in part by the scholarship from China Scholarship Council (CSC) under the Grant No. 201408320149.

REFERENCE

[1] T.Y. Sung, Vibration in semi-infinite solids due to periodic surface loadings, Symp. Dyn. Test Soil. 156(1) (1953) 35-64.
[2] I. Anam, J.M. Roësset, Dynamic stiffnesses of surface foundations: an explicit solution, Int. J. Geomech. 4(3) (2004) 216-223.
[3] G.B. Warburton, J.D. Richardson, J.J, Webster. Forced vibrations of two masses on an elastic half space, J. Appl. Mech., ASME, 38 (1971) 148-156.
[4] J.E. Luco, R.A. Westmann, Dynamic response of a rigid footing bonded to an elastic half-space, J. Eng. Mech. Div. ASME. 39(2) (1972) 527-534.
[5] X.H. Ma, Y.M. Cheng, S.K. Au, Y.Q. Cai, C.J. Xu, Rocking vibration of a rigid strip footing on saturated soil, Comput. Geotech. 36(6) (2009) 928-933.
[6] J. Wang, D. Zhou, W.Q. Liu, S.G. Wang, Rocking response of a surface-supported strip foundation under a harmonic swaying force, Appl. Mech. Mat. 226(2012) 1453-1457.
[7] J. Wang, S.H. Lo, D. Zhou. Frequency-dependent Impedance of a Strip Foundation Group and its Representation in Time Domain. Appl Math Model (2014) DOI:10.1016/j.apm.2014.10.062.
[8] G. Lin, Z. Han, H. Zhong, S.G. Wang, D.S. Du, A precise integration approach for dynamic impedance of rigid strip footing on arbitrary anisotropic layered half-space, Soil Dyn. Earthq. Eng. 49(1) (2013) 96-108.
[9] S.A. Savidis, T. Richter, Dynamic interaction of rigid foundations, in: Proceedings of the 9th International Conference on Soil Mechanics and Foundation Engineering, Tokyo, Japan, 1977, pp: 369-374.
[10] Y. Wang, R. Rajapakse, A.H. Shah, Dynamic interaction between flexible strip foundations, Earthq. Eng. Struct. Dyn. 20(5) (1991) 441-454.
[11] T. Senjuntichai, W. Kaewjuea, Dynamic response of multiple flexible strips on a multi-layered poroelastic half-plane, J. Mech. Mat. Struct. 3(10) (2008) 1885-1901.

APPENDIX

The expressions of the elements in the matrix of Eq. (11):

$$A_{ij}^{(1)}=\frac{-1}{\pi G}\int_0^{\infty}\frac{L_a\sqrt{\eta^2-1}}{2F(\eta)\eta a_0}\left\{\sin\left[\eta\frac{2a_0}{L_a}\left(\frac{(i-j)L_a}{N}+\frac{L_a}{2N}\right)\right]-\sin\left[\eta\frac{2a_0}{L_a}\left(\frac{(i-j)L_a}{N}-\frac{L_a}{2N}\right)\right]\right\}d\eta$$

$$B_{ij}^{(1)}=\frac{-1}{\pi G}\int_0^{\infty}\frac{L_a\sqrt{\eta^2-1}}{2F(\eta)\eta a_0}\left\{\sin\left[\eta\frac{2a_0}{L_a}\left((S+L_b)+\frac{(2i-1)L_a}{2N}-\frac{(j-1)L_b}{M}\right)\right]-\sin\left[\eta\frac{2a_0}{L_a}\left((S+L_b)+\frac{(2i-1)L_a}{2N}-\frac{jL_b}{M}\right)\right]\right\}d\eta$$

$$C_{ij}^{(1)}=\frac{-1}{\pi G}\int_0^{\infty}\frac{L_a\left(2\eta^2-1-2\sqrt{\eta^2-\vartheta^2}\sqrt{\eta^2-1}\right)}{2F(\eta)a_0}\left\{\cos\left[\eta\frac{2a_0}{L_a}\left(\frac{(i-j)L_a}{N}+\frac{L_a}{2N}\right)\right]-\cos\left[\eta\frac{2a_0}{L_a}\left(\frac{(i-j)L_a}{N}-\frac{L_a}{2N}\right)\right]\right\}d\eta$$

$$D_{ij}^{(1)}=\frac{-1}{\pi G}\int_0^{\infty}\frac{L_a\left(2\eta^2-1-2\sqrt{\eta^2-\vartheta^2}\sqrt{\eta^2-1}\right)}{2F(\eta)a_0}\left\{\cos\left[\eta\frac{2a_0}{L_a}\left((S+L_b)+\frac{(2i-1)L_a}{2N}-\frac{(j-1)L_b}{M}\right)\right]-\cos\left[\eta\frac{2a_0}{L_a}\left((S+L_b)+\frac{(2i-1)L_a}{2N}-\frac{jL_b}{M}\right)\right]\right\}d\eta$$

$$A_{ij}^{(2)}=\frac{-1}{\pi G}\int_0^{\infty}\frac{L_a\sqrt{\eta^2-1}}{2F(\eta)\eta a_0}\left\{\sin\left[\eta\frac{2a_0}{L_a}\left(-(S+L_b)+\frac{(2i-1)L_b}{2M}-\frac{(j-1)L_a}{N}\right)\right]-\sin\left[\eta\frac{2a_0}{L_a}\left(-(S+L_b)+\frac{(2i-1)L_b}{2M}-\frac{jL_a}{N}\right)\right]\right\}d\eta$$

$$B_{ij}^{(2)}=\frac{-1}{\pi G}\int_0^{\infty}\frac{L_a\sqrt{\eta^2-1}}{2F(\eta)\eta a_0}\left\{\sin\left[\eta\frac{2a_0}{L_a}\left(\frac{(i-j)L_b}{M}+\frac{L_b}{2M}\right)\right]-\sin\left[\eta\frac{2a_0}{L_a}\left(\frac{(i-j)L_b}{M}-\frac{L_b}{2M}\right)\right]\right\}d\eta$$

$$C_{ij}^{(2)}=\frac{-1}{\pi G}\int_0^{\infty}\frac{L_a\left(2\eta^2-1-2\sqrt{\eta^2-\vartheta^2}\sqrt{\eta^2-1}\right)}{2F(\eta)a_0}\left\{\cos\left[\eta\frac{2a_0}{L_a}\left(-(S+L_b)+\frac{(2i-1)L_b}{2M}-\frac{(j-1)L_a}{N}\right)\right]-\cos\left[\eta\frac{2a_0}{L_a}\left(-(S+L_b)+\frac{(2i-1)L_b}{2M}-\frac{jL_a}{N}\right)\right]\right\}d\eta$$

$$D_{ij}^{(2)}=\frac{-1}{\pi G}\int_0^{\infty}\frac{L_a\left(2\eta^2-1-2\sqrt{\eta^2-\vartheta^2}\sqrt{\eta^2-1}\right)}{2F(\eta)a_0}\left\{\cos\left[\eta\frac{2a_0}{L_a}\left(\frac{(i-j)L_b}{M}+\frac{L_b}{2M}\right)\right]-\cos\left[\eta\frac{2a_0}{L_a}\left(\frac{(i-j)L_b}{M}-\frac{L_b}{2M}\right)\right]\right\}d\eta$$

$$A_{ij}^{(3)}=-C_{ij}^{(1)}$$

$$B_{ij}^{(3)}=-D_{ij}^{(1)}$$

$$C_{ij}^{(3)}=\frac{-1}{\pi G}\int_0^{\infty}\frac{L_a\sqrt{\eta^2-\vartheta^2}}{2F(\eta)\eta a_0}\left\{\sin\left[\eta\frac{2a_0}{L_a}\left(\frac{(i-j)L_a}{N}+\frac{L_a}{2N}\right)\right]-\sin\left[\eta\frac{2a_0}{L_a}\left(\frac{(i-j)L_a}{N}-\frac{L_a}{2N}\right)\right]\right\}d\eta$$

$$D_{ij}^{(3)}=\frac{-1}{\pi G}\int_0^{\infty}\frac{L_a\sqrt{\eta^2-\vartheta^2}}{2F(\eta)\eta a_0}\left\{\sin\left[\eta\frac{2a_0}{L_a}\left((S+L_b)+\frac{(2i-1)L_a}{2N}-\frac{(j-1)L_b}{M}\right)\right]-\sin\left[\eta\frac{2a_0}{L_a}\left((S+L_b)+\frac{(2i-1)L_a}{2N}-\frac{jL_b}{M}\right)\right]\right\}d\eta$$

$$A_{ij}^{(4)}=-C_{ij}^{(2)}$$

$$B_{ij}^{(4)}=-D_{ij}^{(2)}$$

$$C_{ij}^{(4)}=\frac{-1}{\pi G}\int_0^{\infty}\frac{L_a\sqrt{\eta^2-\vartheta^2}}{2F(\eta)\eta a_0}\left\{\sin\left[\eta\frac{2a_0}{L_a}\left(-(S+L_b)+\frac{(2i-1)L_b}{2M}-\frac{(j-1)L_a}{N}\right)\right]-\sin\left[\eta\frac{2a_0}{L_a}\left(-(S+L_b)+\frac{(2i-1)L_b}{2M}-\frac{jL_a}{N}\right)\right]\right\}d\eta$$

$$D_{ij}^{(4)}=\frac{-1}{\pi G}\int_0^{\infty}\frac{L_a\sqrt{\eta^2-\vartheta^2}}{2F(\eta)\eta a_0}\left\{\sin\left[\eta\frac{2a_0}{L_a}\left(\frac{(i-j)L_b}{M}+\frac{L_b}{2M}\right)\right]-\sin\left[\eta\frac{2a_0}{L_a}\left(\frac{(i-j)L_b}{M}-\frac{L_b}{2M}\right)\right]\right\}d\eta$$

where， a_0 is the dimensionless frequency $a_0=\omega L_a/(2V_s)$.